MAGNETITE IN GLASSY MATRIX

V. Sandu[1*], M. S. Nicolescu[1], V. Kuncser[1], I. Ivan[1], E. Sandu[2]
[1] Department of Magnetism and Superconductivity, National Institute of Materials Physics, Magurele, Romania, [2] Department of Life and Environmental Sciences, Horia Hulubei National Institute of Nuclear Physics and Engineering, Magurele, Romania
* Corresponding author(vsandu@infim.ro)

Keywords*: magnetite, glass ceramic, nanostructure, magnetic susceptibility, nucleators, Mössbauer spectroscopy*

1 Introduction

The crystallization of glasses leads to the formation of a special class of nanocomposites consisting of tiny single crystals embedded in a glassy matrix. The process offers the possibility to obtain a new class of nanostructured materials in which the properties of the nanocrystalline phase can be modified by appropriate use of nucleators, composition of the glass matrix and heat treatments [1-4]. Among these vitreous composites, glass–crystalline materials with magnetic phases [3–6] are of special interest due to a large field of technological applications which spans from magnetic storage devices (considered as an ideal 3D magnetic storage medium, because of the high coercivity) to medicine (magnetic hyperthermia, MRI contrasting agents, magnetofectia, biodetection, etc). It is the result of the high suppleness of this method which allows the fabrication of materials with a large variety of shapes and magnetic properties, chemical durability, and biocompatibility. Generally, these composites are obtained starting from a polynar glass melt in which the ingredients must be carefully chosen. It involves an appropriate choice of the glass composition because most magnetic ions occurs in melts in polyvalent state, and the resulting nanocrystalline magnetic phases must comply with special prerequisite valence state. It is also dependent on the choice of the nucleators which control the process of crystal formation and growth. In addition, the thermal excursions during crystallization have also a crucial role in the development of uniformly dispersed single magnetic phase.

There are many magnetic materials with special properties obtained in this way, we mention here Li-ferrites ($LiFe_5O_8$ [7]) $BaFe_{12-2x}Ti_xCo_xO_{19}$ [5, 8-10]) Ca-Ferrite ($Ca_2Fe_2O_5$ [11]), Co-ferrite ($Co_xFe_{3-x}O_4$ [12]), $BaFe_{12}O_{19}$ [13, 14], YIG ($Y_3Fe_5O_{12}$) [15], $SrFe_{12}O_{19}$ [16] etc. However, most investigations of the nanostructured glass-ceramices were dedicated to magnetite Fe_3O_4, which is the unique material accepted for in-vitro application

When the desired magnetic phase is magnetite, Fe_3O_4, the problem of the ratio of the Fe cations is more complex because it requires a minute equilibrium between Fe^{2+} and Fe^{3+} ions in order to obtain the perfect occupation of both tetrahedral and octahedral sites. Generally, both ions exists in the glass melt in equilibrium with the physically dissolved oxygen, but in the redox equilibrium must be also introduced the rest of ingredients which are present in the glass melt.

In our contribution we present the effect of Cr_2O_3 and P_2O_5 as nucleators in conjunction with Al_2O_3 as intermediate in the growth of magnetite nanocrystals within a borosilicate glassy matrix as well as their effect on the magnetic response of the composites.

2 Experimental

Two series of composites with magnetite nanocrystals dispersed within a borosilicate glassy matrix were obtained by crystallization from iron containing borosilicate glass melts. One series has the composition $28.6B_2O_3$ $6.4Na_2O$ $17.5Fe_2O_3$ $(47.5-x)SiO_2$ xNu, i.e., samples C1 and P1, and the second series has the composition $26.8B_2O_3$, $6.4Na_2O$ $24.5Fe_2O_3$ $(40.5-x-y)SiO_2$ yAl_2O_3 xNu, samples C2 and P2. *Nu* stands for nucleator C for Cr_2O_3 and P for P_2O_5, with $x = 0.5$ $y = 3.5$ when $Nu \equiv Cr_2O_3$ whereas $x = 1$, $y = 0$ for P_2O_5.

Each mixture of oxides was melted in preheated alumina crucibles in contact with air and maintained for 2.5 hours at 1470 °C (3 hours for C1 at 1430 °). The melt was cast on a steel mould and the glass slabs were thermally treated at 560 °C for two hours except the sample C2 where the presence of alumina required a longer time for treatment (6 hours). The

treatment temperature was chosen to be 50 °C higher than the dilatometric glassy temperature.
The crystalline phases and their intimate structure were identified by transmission electron microscopy (TEM), electron backscatter diffraction (EBSD), X-ray diffraction, and Mössbauer spectroscopy. For magnetic investigation it was used a SQUID magnetometer (Quantum Design).

3. Results and Discussion

X-ray diffraction data show an intensive process of crystallization of magnetite in all samples attesting the efficiency of both Cr_2O_3 and P_2O_5 as nucleating agents. Traces of ε-Fe_2O_3 and α-Fe_2O_3 are present only in one sample C1. Fig. 1 shows the data for the the latter sample C1 which is more complex. The rest of the samples shows only magnetite.

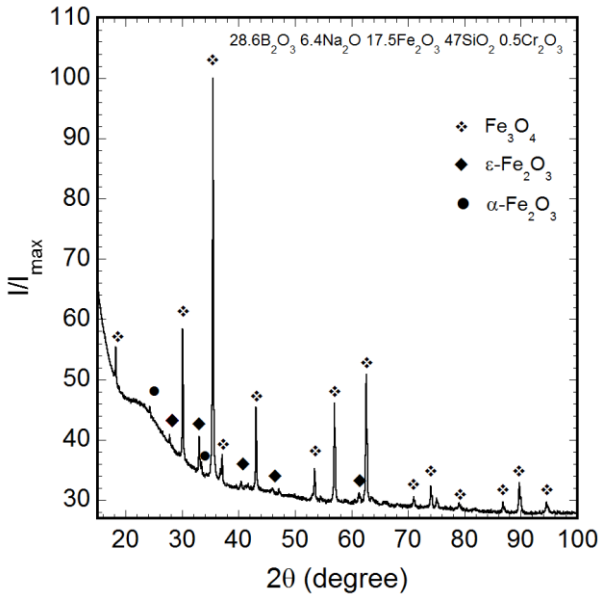

Fig. 1. X-ray diffraction curves of the magnetite-based glass ceramic sample C1.

The degree of crystallinity is 52.4% and 73.1% for C1 and C2, respectively. In the case of P_2O_5 doped samples it is lower: 38.2 % and 45.1% for the samples P1 and P2 respectively.
A EBSD image of the composite sample C1 is presented in Fig. 2. It shows uniformly distributed single crystals within the glassy matrix which is also confirmed by TEM micrographs (Fig. 3). In the rest of the samples, the grains are rather large and made of agglomeration of tiny nanocrystals (fig. 4-6). The average size of the nanocrystals is two times smaller in the samples with P_2O_5 than in the samples with Cr_2O_3, specifically, 33 nm for P1 and 26 nm for P2.

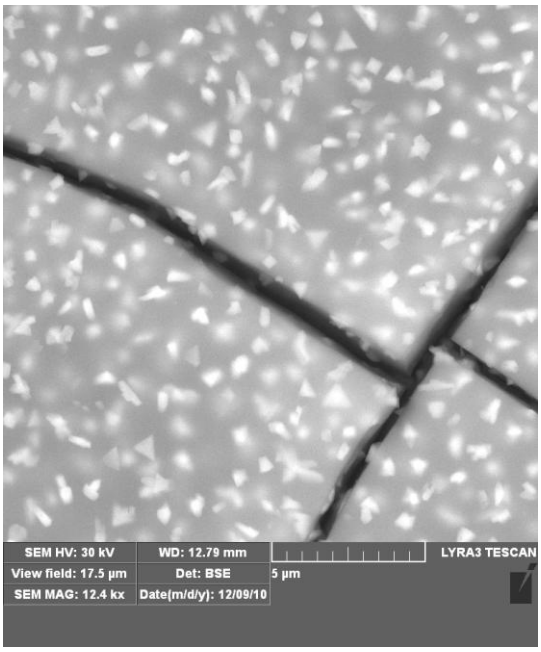

Fig. 2. EBDS image of the composite C1. The single crystals of magnetite are embedded in the glassy matrix.

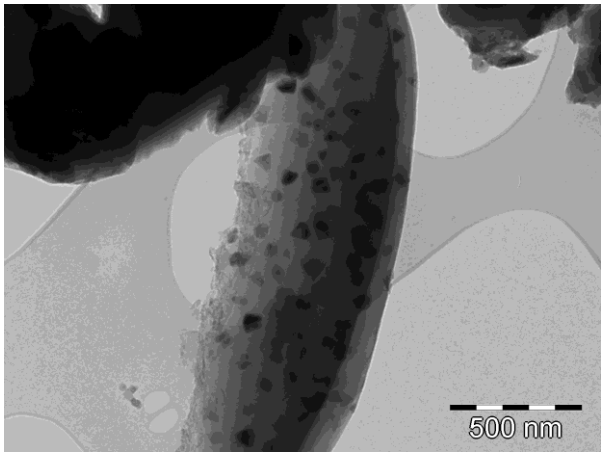

Fig. 3. TEM micrographs of glass ceramic samples C1.

As Mössbauer data show, the reduced degree of crystallinity in the samples P1 and P2 is consistent with the high amount of the Fe ions left dispersed within the glassy matrix as paramagnetic Fe, up to 41 % in the sample P2, whereas in the sample C2 only 16 % of Fe ions is present in paramagnetic state. The magnetic response is strongly influenced

by the structure and only partially can be explained by morphology and diffraction data.

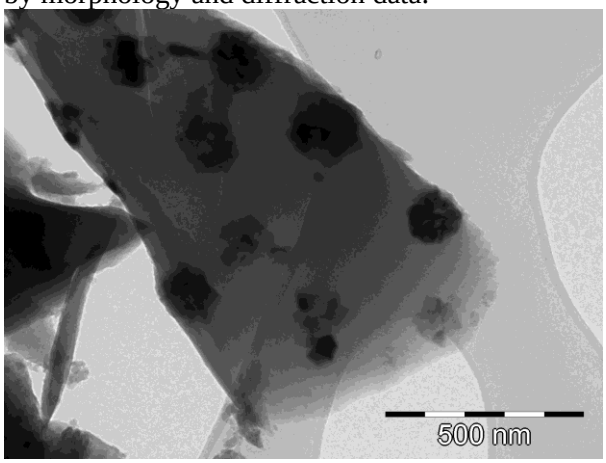

Fig. 4. TEM micrographs of glass ceramic samples C2.

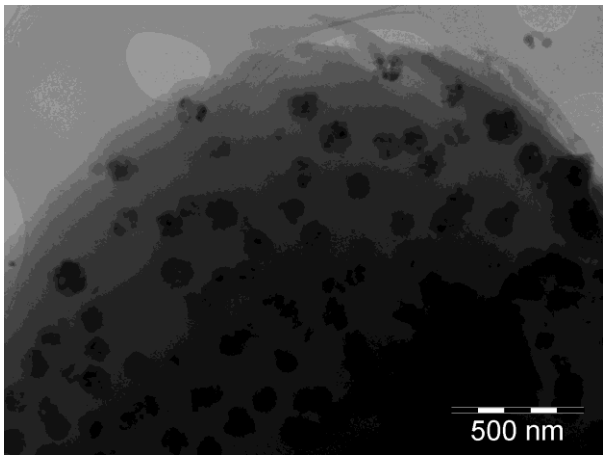

Fig. 5. TEM micrographs of glass ceramic samples P1.

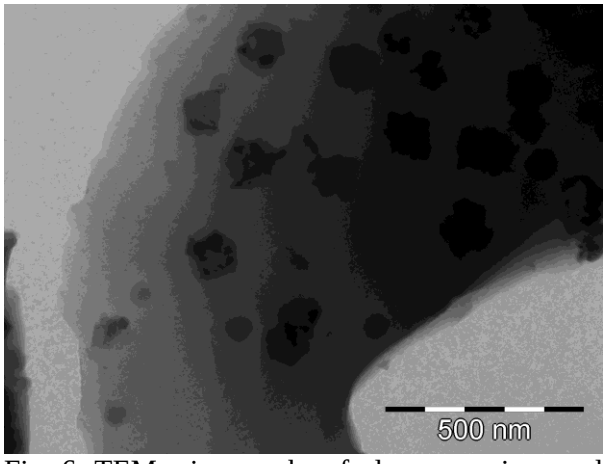

Fig. 6. TEM micrographs of glass ceramic samples P2.

The dynamic of the magnetic particles systems as reflected in χ'(T) and χ"(T) data is very different from sample to sample despite a long series of apparent structural and morphologic similarities between them. Data were collected on warming from 5 to 150 K. Fig. 7 shows the *ac*-susceptibility data for the sample C1. The result is almost typical for nanoparticles, i.e., it displays maxima for both χ'(T) and χ"(T) which shifts to higher temperatures with increasing frequency [17]. However, the shift of the peak of χ'(T) with frequency is too small hence and cannot be attributed to any kind of activated process. Therefore, we cannot attribute the peak to the blocking temperature but to Verwey temperature T_V (90.4 K at 30 Hz). It is to mention that the average crystallite size is rather large, 120 nm. A low temperature shoulder is also present in χ" around 23 K. Bałanda *et al*. [18] considered it as a

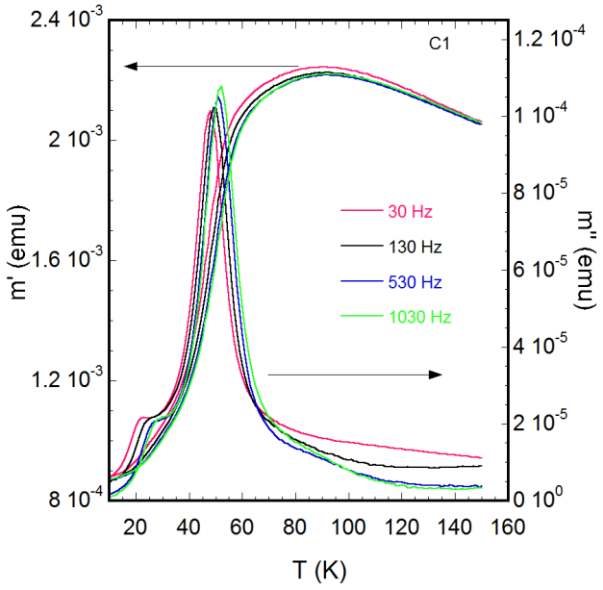

Fig. 7. Temperature dependence of the *ac*-magnetic susceptibility for the sample C1 for frequencies between 30 and 1030 Hz.

result of the electronic processes following the domain relaxation (incoherent tunneling between Fe^{+2} and Fe^{+3}, Fe^{+2} excitation). However, the frequency dependence is not consistent with this picture. The main peak of χ" is the result of the rotation of the magnetic moments and the change of the ionic order within walls. It gives rise to friction which is mirrored in the increase of χ". However, the analysis of frequency shift of the main peak of χ" in terms of Arrhenius dependence leads also to an

abnormally small attempt time, $\tau_0 \sim 10^{-23}$ s [19]. In addition the height of the peak increases with increasing frequency.

Mössbauer spectroscopy (data presented elsewhere [20]) gives $R = 2.1$ for the ratio of the occupied sites within octahedral and tetrahedral positions as obtained via the relative spectral areas of the two magnetic sextets. This value indicates a underoccupation of the tetrahedral sites (in ideal magnetite $R = 2$).

The sample C2 (Fig. 8) shows a clear Verwey transition at $T_V = 116$ K at 30 Hz. but the frequency dependence is even slower than in the previous case. As about χ" it decreases with the frequency, the shoulder at low temperatures evolves to a peak (21.12 K at 30 Hz) but a second shoulder is present at high temperatures (85 K at 30 Hz).

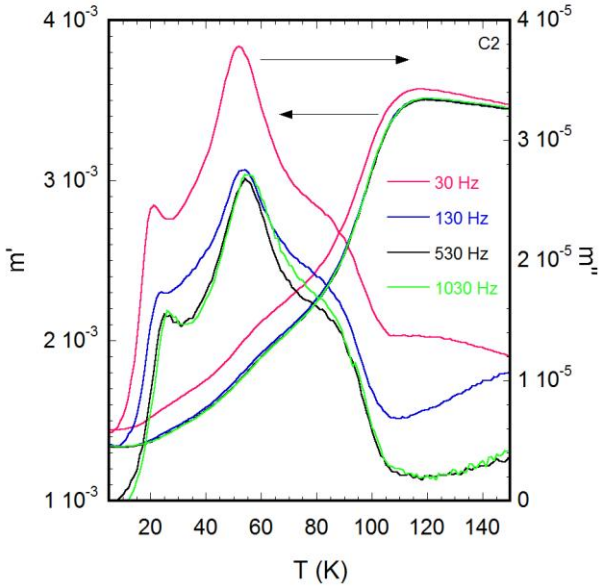

Fig. 8. Temperature dependence of the *ac*-magnetic susceptibility for the sample C2 for frequencies between 30 and 1030 Hz.

In this case, Mössbauer spectroscopy data shows an opposite situation: the octahedral sites are underoccupied because $R = 1.7$.

Both in the case of sample C1 and C2, the hyperfine field remains close to 46 T suggesting the presence of equal occupation of the octahedral sites with Fe^{2+} and Fe^{3+}.

The sample P1 shows a sharp Verwey transition at $T_V = 122$ K followed by a second transition at 39 K where the dissipation (χ") reaches its peak. In this case the frequency shift is negligible (Fig.9).

This sample show a similar underoccupation of the octahedral sites like the sample C2 ($R = 1.7$). It is noteworthy that the amplitude of χ" decreases with frequency in these two cases.

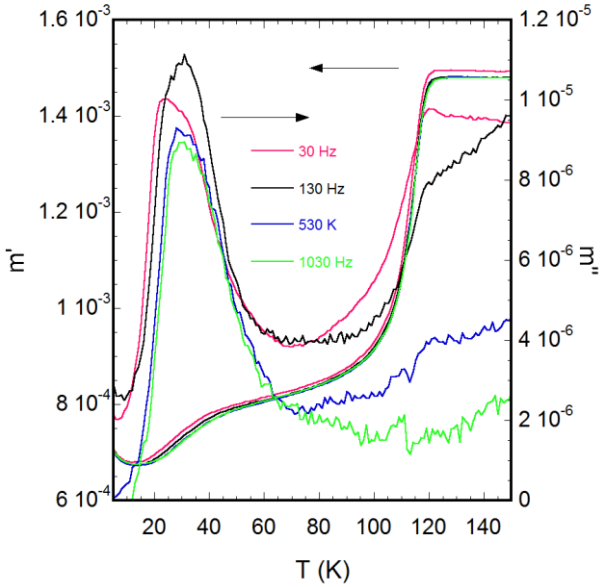

Fig. 9. Temperature dependence of the *ac*-magnetic susceptibility for the sample P1 for frequencies between 30 and 1030 Hz.

The sample P2, which has grains made of small sized nanocrystals (26 nm) has a transition at $T_V = 112$ K at 30 Hz .

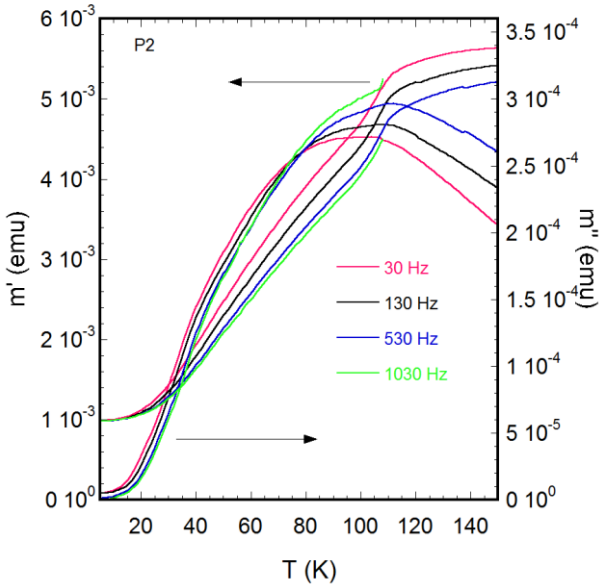

Fig. 10. Temperature dependence of the *ac*-magnetic susceptibility for the sample P2 for frequencies between 30 and 1030 Hz.

What is interesting, χ" is largewide with the peak slightly lower than TV (104 K at 30 Hz) and amplitudes that increases with the frequency (like in the case of the sample C1). The grain size suggests the possibility of single domain crystallites since the limit of single domain grains is $d_c = 3.6\sqrt{\frac{2A}{4\pi m_s^2}} = 29.7$ nm [21]. Here A is the exchange stiffness constant and m_s the saturation magnetization.

For this composite, Mössbauer data are consistent with almost perfect magnetite from occupation point of view with $R = 2$. However, this sample has also a strong paramagnetic contribution resulting from the huge amount of Fe ions dispersed in the vitreous matrix (75% as Fe^{3+}).

It is also noteworthy the fact that for this sample, with $R = 2$, as well as for the sample C1, with $R = 2.1$, the amplitude of the peak of χ" increases with increasing the frequency.

In conclusion, the composites with magnetite embedded in vitreous matrix display complex magnetic responses which depend on the degree of vacancies in the structure of magnetite as well as on the location of these vacancies within the two sublattices. However, the problem is more complex and a clear response would require also the analysis of the role of the structural and ferroelastic domains in the dynamic behavior.

Acknowledgments

This work was supported by the Romanian NASC under the Project PN II-72-151/2008

References

1. Z. Strnad, Glass–Ceramic Materials, Elsevier, Amsterdam, 1986.
2. R. Müller, R. Hiergeist, H. Steinmetz, N. Aqoub, M. Fujisaka, W. Schüppel, J. Magn. Magn. Mater., 201 (1999) 34.
3. P. A. Mariño-Castellanos, J. C. Somarriba-Jarque, J. Anglada-Rivera, Physica B 362 (2005) 95
4. D. D. Zaitsev, P. E. Kazin, A. V. Garshev, Yu. D. Tret'yakov, and M. Jansen, Inorg. Mater., 40 (2004). 881
5. Y.-K. Lee and S. Y. Choi, J. Am. Ceram. Soc. 79 (1996) 992.
6. P. Görnert et al., IEEE Trans. Magn. 26 (1990) 12
7. N. Rezlescu, E. Rezlescu, P. Pasnicu, M.L. Crans, J. Magn. Magn. Mater. 131 (1994) 274.
8. B. T. Shirk, W. R. Buesseln, J. Am. Ceram. Soc. 53 (1970) 192.
9. W. J. S. Blackburn, B. P. Tilley, J. Mater. Sci. 9 (1974) 1265.
10. Th. Klupsch, E. Steinbeiss, R. Müller, C. Ulbricht, W. Schüppel, H. Steinmetz, T. Höche, J. Magn. Magn. Mater. 196&197 (1999) 264.
11. Tetsuaki Nishida, Shiro Kubuki, Morihiro Shibata, Yonezo Maeda and Toyomi Tamaki , J. Mater. Chem., 7 (1997) 1801
12. R. Müller and W. Schüppel, J. Magn. Magn. Mater., 155 (1996) 110
13. M. Pal, P. Brahma, D. Chakravorty, D. Bhattacharyya, H. S. Maiti, Nanostructured Materials 8, (1997) 731
14. G. J. Chen, L. Y. Jian, Y. S. Chang, C. Y. Chung and Y. L. Chai, J..Cryst. Growth, 277 (2005), 457
15. G. J. Chen, H. M. Lee, Y. S. Chang, Y. J. Lin, Y. L. Chai, J. Alloys Comp. 388 (2005) 297
16. D. D. Zaitsev, P. E. Kazin, Yu. D. Tret'yakov, Yu. V. Maksimov, I. P. Suzdalev and M. Jansen, Inorg. Mater. 40 (2004) 1111
17. J. L. Dormann, D. Fiorani, and E. Tronc, Adv. Chem. Phys. XCVIII (1997) 326
18. M. Bałanda, A. Wiecheć, D. Kim, Z. Kąkol, A. Kozłowski, P. Niedziela, J. Sabolb, Z. Tarnawski, and J.M. Honig, Eur. Phys. J. B 43 (2005) 201
19. J. L. Dormann, D. Fiorani, and E. Tronc, J. Magn. Magn. Mater. 202 (1999) 251
20. V. Sandu, M. S. Nicolescu, V. Kuncser, S. Popa, I. Pasuk, C. Ghica, and E. Sandu, J. Nanosci. Nanotechnol. (accepted)
21. W. F. Brown Jr., J. Appl. Phys. 39 (1968) 993